Sādhanā (2022)47:36
https://doi.org/10.1007/s12046-021-01791-1

Thermodynamic analysis of sensible heat storage based double pass hybrid solar air heater with and without reflector

OM PRAKASH[1,*], ANIL KUMAR[2,3,*] and VINOD LAGURI[4]

[1]Department of Mechanical Engineering, Birla Institute of Technology, Mesra, Ranchi, India
[2]Department of Mechanical Engineering, Delhi Technological University, Delhi, India
[3]Centre for Energy and Environment, Delhi Technological University, Delhi, India
[4]Department of Mechanical Engineering, Indian Institute of Science (IISc), Bangalore, India
e-mail: 16omprakash@gmail.com; anilkumar76@dtu.ac.in; vinodlaguri@iisc.ac.in

MS received 1 June 2021; revised 29 November 2021; accepted 8 December 2021

Abstract. Solar air heater or solar heating system is a very useful solar thermal product used for multiple purposes such as drying, space heating, desalination, and various industrial applications for low temperature. In this communication, a comprehensive study on the energy-exergy analysis of sensible heat storage based on double pass solar air heater with and without the reflector. System is manufactured with locally available materials. Heat storage material (Metco material and aluminium scrap mixture) was used under the bottom layer. Three cases of experiments were planned, namely natural mode (case 1), double pass solar heater (case 2) and double pass solar air heater with reflector (case 3). Case 3 shows the superior thermal performance as compared to case 1 and 2. The outlet temperature varies from 36 to 60°C; 35 to 58.20°C and 38.5° to 73.2°C in Cases 1, 2 and 3, respectively. This was mainly due to the application of the reflector. It provided additional input energy to the solar air heater.

Keywords. Double pass; solar air heater; reflector; sensible thermal storage.

1. Introduction

Solar air heater is a multipurpose device used in various applications such as drying and space heating. This work is based on the greenhouse effect and utilizes solar radiation's heat to heat the flowing air [1, 2]. Its conversion efficiency is higher than solar photovoltaic panels. There are three major parts for the solar air heater or solar air heating system: close box with inlet and outlet holes, top transparent glass, and absorber plate [3]. Intense research work is happening in the field of solar air heaters to improve the performance and reduce cost by modification in its design, change of material for absorber plate and structure [4].

Initially, the system was developed as Single Pass Solar Air Heater (SPSAH). Inlet air comes from the downward side, which gets heated up due to greenhouse effect and exhaust is through outlet vent. The system can be operated in both active and passive modes [5]. For higher mass flow rate, researchers prefer to use active mode based system. To take full advantage of the available heat, Double Pass Solar Air Heater (DPSAH) is being first developed by Satcunanathan and Deonarine [6]. In this concept, top loss from transparent glass to surrounding is being minimized greatly. The system can be operated in both active and passive however for better performance active mode is preferred.

In comparison with performance of DPSAH with SPSAH, the outlet temperature is much higher in SPSAH. Here the secret of success is due to contact of flowing inside air to the top and bottom of the absorber plate. However, in the SPSAH, the flow air contact only on the top of the absorber plate. The curved type DPSAH is studied by Kumar *et al* [7]. Various designs of this system are being investigated in this study. Asymmetric semi-circular ribs in the system have the highest thermo-hydraulic performance compared to other types of DPSAH. It is also suggested that absorber plate of the DPSAH should be kept at the middle of the inlet and outlet duct. It was also found that asymmetric semi-circular ribs show better efficiency than symmetric circular ribs. A study had been carried out by Yeh *et al* [8] on innovative DPSAH. In this system, fins are attached on both sides of the absorber plate. There is a significant increase in the overall efficiency of the proposed system as compared to the SPSAH.

An innovative solar DPSAH is being investigated by Ho *et al* [9]. In this system, baffles and fins are attached to the DPSAH. Due to this, more heat exchange happens between the absorber plates to the flowing air. This leads to significant improvement in the overall thermal efficiency of the system as compared to the SPSAH.

*For correspondence
Published online: 12 February 2022

A DPSAH with mixed thermal heat storage (paraffin wax with foam aluminium) had been studied experimentally by Baig and Ali [10]. The experiment is conducted in four different conditions. In first condition, there is no storage concept applied in the DPSAH; however, in the second condition, aluminium and paraffin wax were kept inside the two cooper tubes, in third condition, same as second condition except for four storage based copper tube and in fourth condition, same as third case except no induced fan is used. Study shows that in the fourth condition, system works 2. 5 hours more after off sunshine hour, which is highest in all the cases.

Vijayan *et al* [11] studied the sensible thermal storage concept based on solar heating systems or solar air heaters. In the system, absorber plate is of corrugated shape and storage materials applied on it. Energy efficiency of the storage bed varies from 20.35% to 50.92.% and exergy efficiency vary from +3.97% to −2.81% when air mass flow rates vary from 0.0141 kg/s to 0.0872 kg/s. Energy efficiency of the proposed system is 3-8% higher than without storage system operating under the same condition. The outlet air temperature from system varies from 45°C to 60°C, which is appropriate for various applications such as drying and space heating.

Kalaiarasi *et al* [12] studied the comparative study of solar heating systems with and without sensible thermal storage material. Therminol-55 material is used as storage material for this system. Proposed system is operated in three different quantities namely 0.017, 0.02 and 0.028 kg/s. The maximum outlet air temperature (97°C) is obtained at 0.017 kg/s and minimum outlet temperature at 0.028 kg/s. The efficiency of the storage based system has higher thermal efficiency as compared to the without storage system.

After intense literature review, some research work was found in the field of double pass solar air heater assisted with the thermal storage material. However, there is no literature on the thermodynamic analysis of DPSAH with sensible thermal storage assisted stainless steel reflector.

Hence, main objective of present work is to compare the performance of DPSAH with sensible storage material between with and without reflector. To achieve the desired objective, cost effective proposed system is designed and developed with locally available material. In the first section of the article, the experimentation of the proposed system is being conducted in three different cases; namely, natural mode, induced forced mode and induced forced mode coupled with reflector. Uncertainty analysis of the experimental data has been done. Second section deals with the energy and exergy analysis of the experimental data. Lastly, thermal efficiency was being compared with previously published literature, and results of the proposed system were found to be superior compared to other systems. The conclusions are provided at the end.

2. Material and method

2.1 *Experiment setup*

The experimental setup was used in this study is shown in figures 1, 2 and 3. This study had three different sets of experiments conducted on three different consecutive days. On Day 1 (case 1) study conducted under natural mode of DPSAH (figure 1). Day 2 (case 2) study had been conducted under induced mode of DPSAH as shown figure 2 and Day 3 (case 3) study had been conducted under induced mode of DPSAH with reflector as shown in figure 3. In all three cases, dimension and materials of DPSAH remain same. In case 2, one induced fan was provided additional to case 1 and case 3, one additional reflector is provided compared to case 2. The external structure of the entire solar heating system was made up of 05 mm thick polycarbonate sheet. Polycarbonate sheet was selected due to its high durability and light weight. Two vents of square type (15×15 cm^2) were provided in the system for the incoming and outgoing air. The absorber plate was located in the middle of two vents. Copper sheet of 02 mm thick was used as absorber plate and it was coated with Aluminium silicon-boron nitride powder. This coating material was selected due to higher heat absorbent capacity. The entire system was well insulated with the help of glass wool so that minimum heat loss happens in side, bottom and edges of the system and top surface of the system was made up of 03 mm thick transparent toughen glass. Toughen glass was used in the place of normal glass due to its enhanced strength. Absorber plate was kept at a distance of 05 mm below the toughen glass. Sensible thermal storage concept was applied beneath the bottom layer of the air heater. Aluminium scrap painted with aluminium silicon boron nitride was used as storage material. Thickness of the storage material is 50 mm and weights 20 kg. This makes it uniform below the bottom layer of the air heater. The thickness of the storage material is selected as per recommendation by Aboul-Enein *et al* [13]. Emissivity and absorptivity of the coated material is higher than conventional black paint. Emissivity and absorptivity for conventional black paint were found to be 0.85 and 0.95; however, for coated material in the proposed study (aluminium silicon-boron nitride) found to be 0.80 and 0.97 as per Duffie and Beckman [14]. Due to this, heat absorption capacity of the absorber plate gets enhanced.

Solar air heating system was kept on the iron frame in the inclined position. The inclination angle which was the latitude angle of Ranchi, India which is 23°. At this inclination, optimum solar radiation is received round the year [11]. Square shaped polished steel of size 0.5×0.5 m^2 was used as reflector. Position of the reflector fixed in the frame can be adjusted according to movement of the sun. Hence, enhancement in the received solar radiation on the proposed system takes place.

The direction of air flow within the system in Case 1 (natural mode) was from top to bottom i.e. comes in the top vent and moves above the absorber plate and flows out under the absorber plate. It comes out from the lower vent. In Case 2 and Case 3, the direction of air flow is just reverse as compared to Case 1. Inlet air comes through the lower vent and gets out through the upper vent. In both cases, exhaust fan is being applied at the outlet vent. DC Fan (18 W) is powered by 40 W polycrystalline solar cell assisted with solar charge controller cum rechargeable battery.

Locally available materials had been used to fabricate in the proposed system in which Polycarbonate sheets hold 15.60 kg. Table 1 represents different components used with their weight in the manufacturing of the proposed system. Contribution of various materials used is presented in figure 4. Embodied energy of various components is used in the proposed system is given in Table 2 and their contribution presented in figure 5, in which Metco material holds highest percentage of 38%. Embodied energy in Case 1 is 681.484 KW/h, in Case 2 is 751.5809 kW/h and in Case 3 is 841.8309 kW/h.

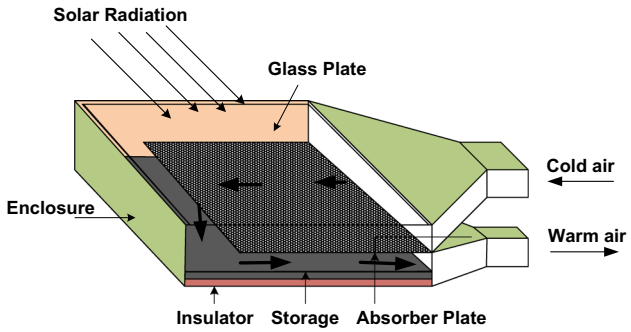

Figure 1. Schematic diagram under natural mode.

Various measuring instruments used in this experiment are given in Table 3 with their specification. Least count of different devices is mentioned in figure 6. In which moist evaporation has the highest least count 0.5 and voltage, current and wind velocity together holding a least count of 0.01 and the values of each is mentioned in Table 4.

2.2 *Methodology*

A. Energy analysis

Energy analysis of the proposed system was conducted with the help of experimental data (figure 6). This analysis is based on the conservation of energy principle. For the present system, the following energy balance equations are used:

$$Q_A = Q_u + Q_{loss} + Q_{st} \tag{1}$$

Now each term can be expressed in the following ways:

The Q_u is expressed as the total amount of heat utilized and which is mathematically expressed as follows (Nidhul *et al* [15]):

$$Q_u = \dot{m}\, C_p (T_{out} - T_{inlet}) \tag{2}$$

Where, m is the MFR of the air inside the system. This can be evaluated by the following expression (Nidhul *et al* [15]):

$$\dot{m} = \rho V_{ai} S \tag{3}$$

In this system, the primary source of energy is solar radiation. The net solar radiation absorbed by the absorber plate is denoted by Q_A which is evaluated by the following expression (Nidhul *et al* [15]):

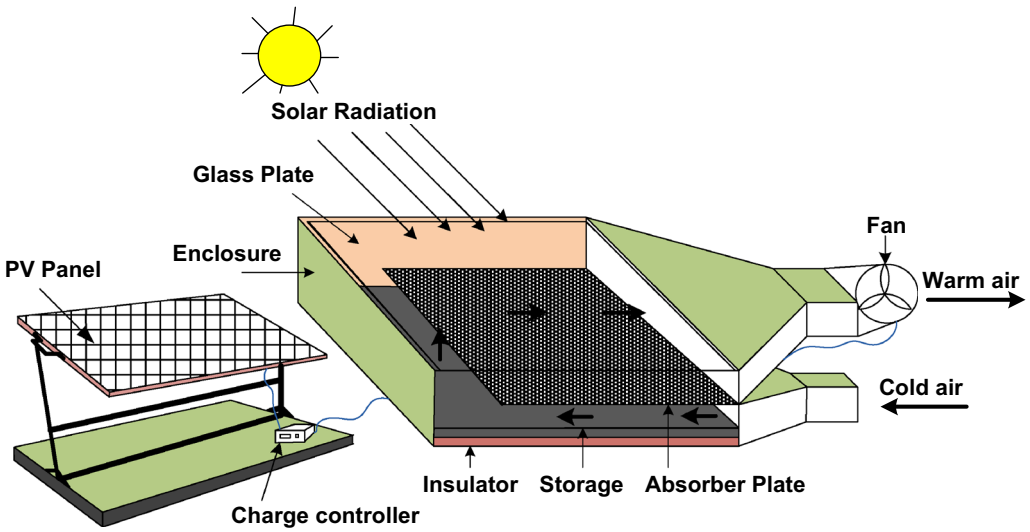

Figure 2. Schematic diagram under induced mode.

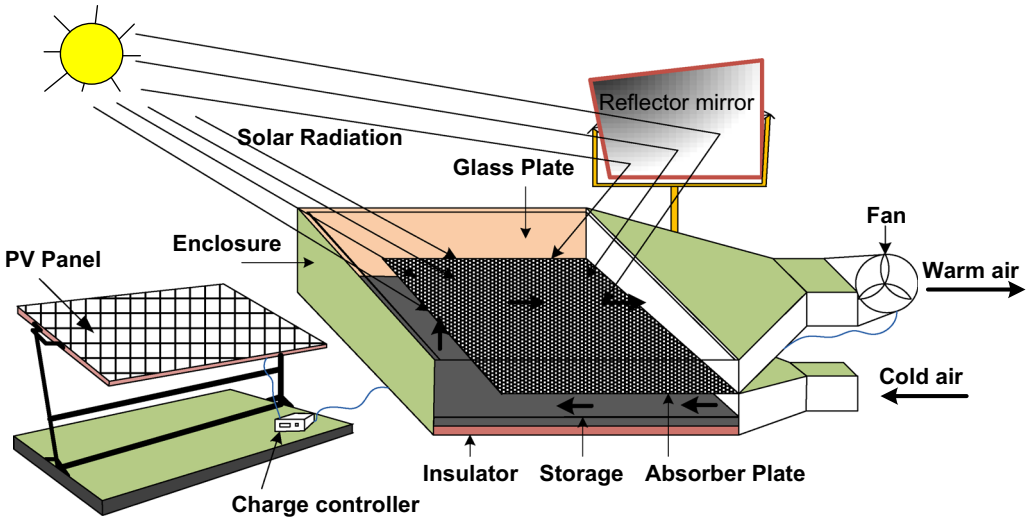

Figure 3. Schematic diagram of the double pass solar air heater with reflector.

$$Q_A = A_{plate}(\alpha\tau)I_i \tag{4}$$

In the solar collector, some heat loss occurs on the bottom side and top surface of the system. Therefore, the total amount of heat loss is calculated by the following expression (Nidhul *et al* [15]):

$$Q_{loss} = U_{loss}A_{plate}(T_{plate} - T_{ambient}) \tag{5}$$

U_{loss} is total heat losses coefficient which include losses from the top (U_{top}), bottom (U_{bot}) and side (U_{side}). Mathematically it is expressed as follows:

$$U_{loss} = U_{side} + U_{bot} + U_{top} \tag{6}$$

Where the parameters are evaluated as Esen [16]:

$$U_{top} = \left[1/(h_{r,Pg} + h_{c,Pg}) + 1/(h_{r,ga} + h_w)\right]^{-1} \tag{7}$$

$$U_{bot} = \lambda_i/\delta_{bot} \tag{8}$$

$$U_{side} = ((L_1 + L_2)L_3\lambda_i)/(L_1L_2\delta_e) \tag{9}$$

The unknown parameters can be evaluated as follow [17–21]:

$$h_{c,pg} = Nu(\lambda/t) \tag{10}$$

$$Nu = 0.68 + \frac{(0.67 \times Ra^{1/4})}{(1 + (0.492/\Pr)^{9/16})^{4/9}} \quad [Ra \le 10^9] \tag{11}$$

$$h_{r,Pg} = \left(\frac{\sigma(T_{ground}^2 + T_{Plate}^2)(T_{ground} + T_{plate})}{\left(\frac{1}{\varepsilon_{plate}} + \frac{1}{\varepsilon_{plate}} - 1\right)}\right) \tag{12}$$

$$h_w = 3.86V_{air} + 5.67 \tag{13}$$

Table 1. Mass of various component used for fabrication of the SAH.

Sl. No	Material	Quantity
1	Glass	5.40 kg
2	Polycarbonate sheet	15.60 kg
3	Black coating	0.75 m^2
4	Copper Sheet	0.30kg
5	Metco Material	12.00 kg
6	Aluminium Scrap	8.00 kg
7	Ceramic Wool	1.00 kg
8	DC fan	
	(I)Plastic	0.120
	(II) Copper wire	0.050
9	Polycrystalline solar cell	0.059 m^2
10	Battery	
11	Solar charge controller	
12	Stainless steel	1 kg
13	Iron	05 kg

$$h_{r,ga} = \varepsilon_g\sigma(T_{ground}^2 + T_{sky}^2)(T_{ground} + T_{sky}) \tag{14}$$

$$T_{sky} = 0.0552T_{ambient}^{1.5} \tag{15}$$

According to the first law of thermodynamics, the thermal efficiency of the SAH is the ratio between the useful energy (Q_u) and the solar radiation received on the collector. Thermal efficiency can be calculated by the Eq. (16) [22, 23]:

$$\eta_{Thermal} = Q_u/I_iA_{plate} \tag{16}$$

The dimensionless parameters referred above are given by Eqs. (17), (18) and (19) [24]

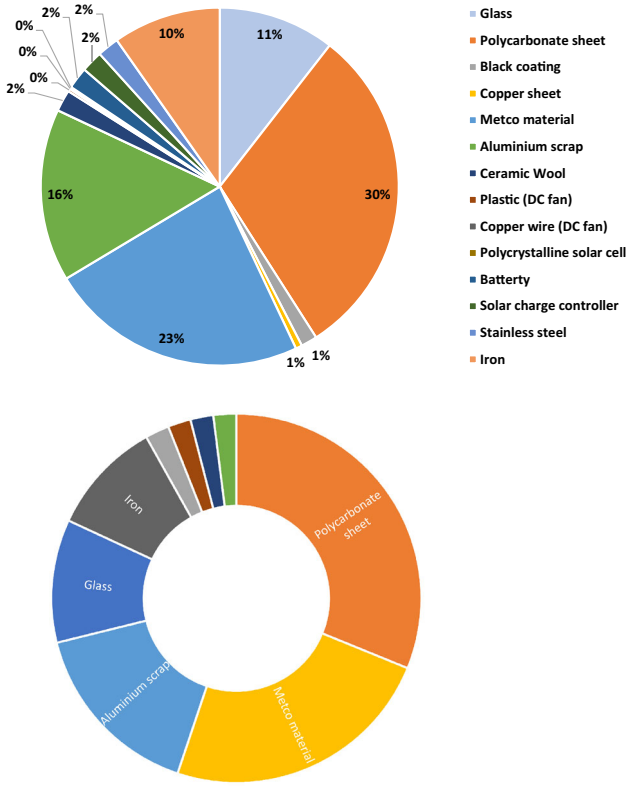

Figure 4. Distribution of different material in construction of solar heating system.

$$Ra = \frac{g\beta\Delta TL^3}{\alpha v} \tag{17}$$

$$\Pr = \frac{v}{\alpha} \tag{18}$$

$$\mathrm{Re} = \frac{V_{air} D_h}{v} \tag{19}$$

B. Exergy analysis of the SAH

Exergy analysis of the proposed system was evaluated based on experimental data. Few assumptions were taken to do the analysis:

a. System is in thermodynamic equilibrium.
b. Inside air flow is of steady-state with constant physical properties along with very small amount of relative humidity.

Exergy balance equation is being developed based on second law of thermodynamics. Exergy at the inlet of the SAH is given as Eq. (20).

$$Ex_{inlet} = Ex_{dest} + Ex_{outlet} + Ex_{stored} + Ex_{lost} \tag{20}$$

Where

Ex_{inlet},$Ex_{dest}Ex_{outlet}Ex_{stored}$ and Ex_{lost} are the various exergy for the inlet flowing air, destroyed, outlet point, stored and lost exergy.

Exergy for inlet airflow is calculated by Eq. (21) [25]:

$$\begin{aligned} &Ex_{inlet}(flowing\ air) \\ &= \dot{m}\, C_P \left(T_{inlet} - T_{ambient} \left(1 + \ln\left(\frac{T_{inlet}}{T_{ambient}} \right) \right) \right) \\ &\quad + \dot{m}\, RT_{ambient} \ln\left(\frac{P_{inlet}}{P_{amb}} \right) \end{aligned} \tag{21}$$

And the exergy at outlet air flow is expressed as Eq. (22) [26]:

$$\begin{aligned} &Ex_{outlet}(flowing\ air) \\ &= -\dot{m} C_P \left(T_{out} - T_{ambient} \left(1 + \ln\left(\frac{T_{out}}{T_{ambient}} \right) \right) \right) \\ &\quad - \dot{m} RT_{ambient} \ln\left(\frac{P_{out}}{P_{amb}} \right) \end{aligned} \tag{22}$$

Table 2. Embodied energy analysis for fabrication of SAH.

Sl. No	Material	Embodied Energy Coefficient	Case 1	Case 2	Case 3
1	Glass	7.28 (KWh/kg)	39.312	39.312	39.312
2	Polycarbonate sheet	10.20 (KWh/kg)	159.12	159.12	159.12
3	Black coating	0.28 (KWh/m^2)	0.21	0.21	0.21
4	Copper Sheet	19.44 (KWh/kg)	5.832	5.832	5.832
5	Metco Material	26.76 (KWh/kg)	321.12	321.12	321.12
6	Aluminium Scrap	18.98 (KWh/kg)	151.84	151.84	151.84
7	Ceramic Wool	4.05 (KWh/kg)	4.05	4.05	4.05
8	DC fan				
	(I)Plastic	19.44 (KWh/kg)	–	2.332	2.332
	(II) Copper wire	19.61 (KWh/kg)	–	0.9805	0.9805
9	Polycrystalline solar cell	1130.60 (KWh/m^2)	–	66.7054	66.7054
10	Battery		–	0.046	0.046
11	Solar charge controller		–	0.033	0.033
12	Stainless steel	55.55 (KWh/m^2)	–	–	55.55
13	Iron	6.94 (KWh/m^2)	–	–	34.70
		Total Embodied Energy (KWh)	681.484	751.5809	841.8309

Exergy for absorbed solar radiation can be calculated as Eq. (23) [27]:

$$Ex_{inlet}(solar\ radiation) = I_i\left[1-\frac{4}{3}\left(\frac{T_{ambient}}{T_{sky}}\right)+\left(\frac{T_{ambient}}{T_{sky}}\right)^4\right] \quad (23)$$

where T_{sky}= 5777 K.

The lost exergy, Ex $_{lost}$ can be indicated as Eq. (24) [28, 29]:

$$Ex_{lost} = -U_{lost}A_{col}[(T_{Plate}-T_{ambient})-(T_{ambient}+273)ln\frac{(T_{Plate}+273)}{(T_{ambient}+273)}] \quad (24)$$

The exergy destruction Ex_{dest} is dependent on three different terms [29]

i. Temperature difference between the absorber plate and sun (shown in Eq. (25)).
ii. Pressure drop at duct as shown in Eq. (26).
iii. Heat transfer to the flowing air from absorber plate to the surface as shown in Eq. (27).

$$Ex_{dest(p-s)} = -\eta_0 I_i A_{col} T_{ambient}\left(\left(\frac{1}{T_{plate}}\right)-\left(\frac{1}{T_{sky}}\right)\right) \quad (25)$$

$$Ex_{dest(\Delta P)} = -(\Delta P T_{ambient}/\rho)\left(_{ambient}\ln\left(\frac{T_{out}}{T_{ambient}}\right)\right)(T)/(T_{out}-T_{inlet}) \quad (26)$$

$$Ex_{dest(p-f)} = -\dot{m}\,C_p T_{ambient}\left(\ln\left(\frac{T_{out}}{T_{inlet}}\right)-\left(\frac{T_{out}-T_{inlet}}{T_{plate}}\right)\right) \quad (27)$$

The daily exergy efficiency of the SAH can be calculated as Eq. (28) [30]

$$\eta_{Exergy} = \left(\int Ex_{out}/\int Ex_{inlet}\right)\times 100\% \quad (28)$$

2.3 *Uncertainty analysis*

Every measuring instrument has limitations; none of the measuring devices is 100% accurate. Uncertainty analysis is intended to indicate the possible error in measurement by the instruments. The uncertainty analysis is being calculated with the help of Eqs. 29–33. Table 2 shows the external Uncertainty Percentage Error.

$$W_Y = \sqrt{\left(\frac{\partial Y}{\partial y_1}W_1\right)^2+\left(\frac{\partial Y}{\partial y_2}W_2\right)^2+\left(\frac{\partial Y}{\partial y_3}W_3\right)^2+\cdots+\left(\frac{\partial Y}{\partial y_n}W_n\right)^2} \quad (29)$$

$$W_{Temp}=\sqrt{(W_{thermometer})^2+(W_{reading})^2} \quad (30)$$

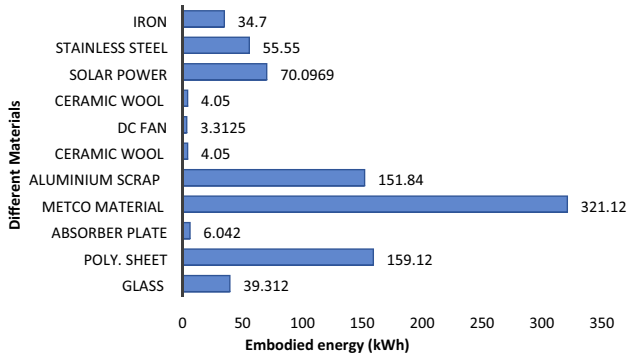

Figure 5. Distribution of embodied energy of different materials.

Table 4. External Uncertainty Percentage Error.

Sl. No	Measurement Error	Value
1	Absorber temperature	0.10
2	Air temperature	0.10
3	Relative humidity	0.10
4	Moisture evaporation	0.50
5	Voltage	0.01
6	Current	0.01
7	Wind velocity	0.01
8	Plate Temperature	0.10
	Total Percent External Uncertainty	0.93

Table 3. Technical instruments and measurement device.

Device	Quantity	Model/Producer	Range	Accuracy
Anemometer	1	Lutron/AM4202	0.4-30 m/s	± 0.1 ms^{-1}
Solar Power Meter	1	CEM/LA-1017	0e1999 W/m^2	±10W/m^2
Thermocouples	8	K-type/ Jain Automation	− 200–1200°C	±0.5°C

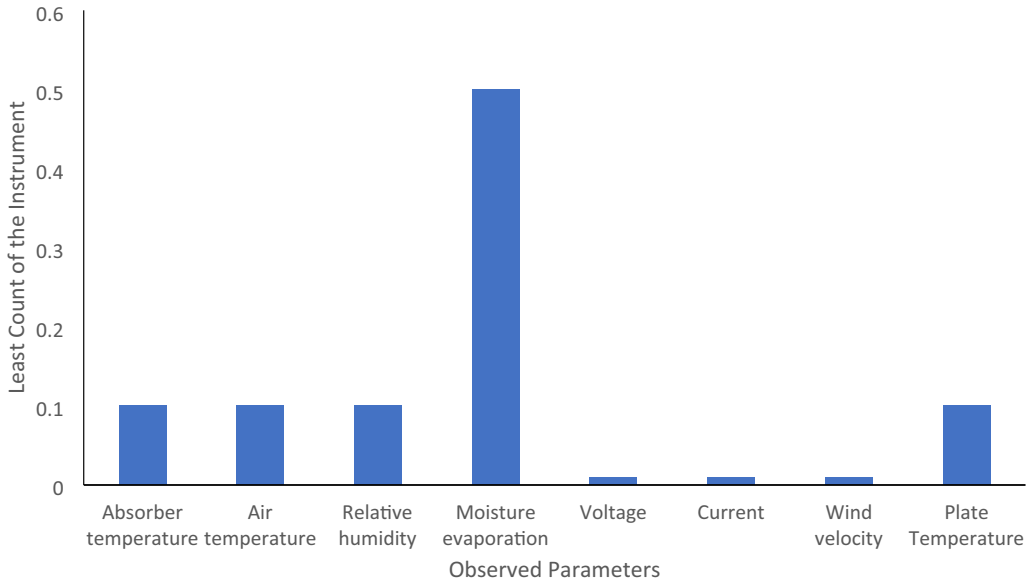

Figure 6. Least count of instruments to major parameters.

$$W_{Wind}=\sqrt{(W_{anemometer})^2+(W_{\text{reading}})^2} \quad (31)$$

$$W_{Radiation}=\sqrt{(W_{Pyranometer})^2+(W_{\text{reading}})^2} \quad (32)$$

$$W_{Exp}=\sqrt{(W_{Wind})^2+(W_{Temp})^2+\ +(W_{Radiation})^2} \quad (33)$$

By solving all these equations Eqs. (30)–(33) with the help of Table 3, total uncertainty is found to be ±0.2004% which is in actable range.

3. Result and discussion

In this section, the discussion on the experimental results and energy-exergy analysis is presented.

3.1 *Experimental results*

The proposed system is being experimented on three consecutive days in three different modes. In case 1 system is in natural mode, case 2 system is in induced mode and case 3 system is induced with reflector mode. In all three cases, ambient parameters were very similar with little variation due to clear sky conditions. Hence comparison of the thermal performance becomes appropriate in the atmospheric condition.

The variation of ambient wind speed in case 1 is 0.22–0.70 m/s; 0.27–0.65 m/s in case 2 and 0.28–0.71 m/s in case 3 as presented in figure 7. Hence average variation in wind speed is less than 10% among all three cases of experimentation.

Various temperature at important location is also measured to evaluate thermal performance of the proposed system. These temperatures are the top glass temperature, absorber plate temperature and outlet temperature in all three cases.

The variation of all the different temperatures (ambient temperature, glass temperature, outlet temperature and plate temperature) depends on solar radiation. The variation of all different temperatures and solar radiation during experimentation in all three cases is shown in figure 8. Experiment was conducted from 9.00 AM to 5.00 PM in all three cases on 10–12 April 2020. The variation of solar radiation on case 1 is 360–950 W/m^2; 355–945 W/m^2 on case 2 and 350–940 W/m^2 on case 3, as presented in figure 8. In all three cases, the maximum solar radiation comes out at 1.00 PM and minimum at 5.00 PM. Hence average variation in global radiation is less than 1% among all three cases of experimentation. The variation of ambient temperature on case 1 is 30°–35.80°C; 26°–40.40°C on case 2 and 25.20°–37.80°C on case 3 as presented in figures 8 and 9. The maximum ambient temperature for case 1 is at 2.00 PM, case 2 is at 2.00 PM, and case 3 is at 1.00 PM. Hence average variation in ambient temperature is less than 10% among all three cases of experimentation.

The variation of top glass temperature on case 1 is 34°–58°C; 31°–45°C on case 2 and 29.5°–65°C on case 3 as presented. The average top glass temperature was found to be lowest in case 2 i.e., 39.33oC; however,in case 3, it was found 54.28°C.

The variation of absorber plate temperature on case 1 is 40°–81°C; 34.5°–70°C on case 2 and 55°–89 ° C on case 3 as presented in figure 8. The average top glass temperature

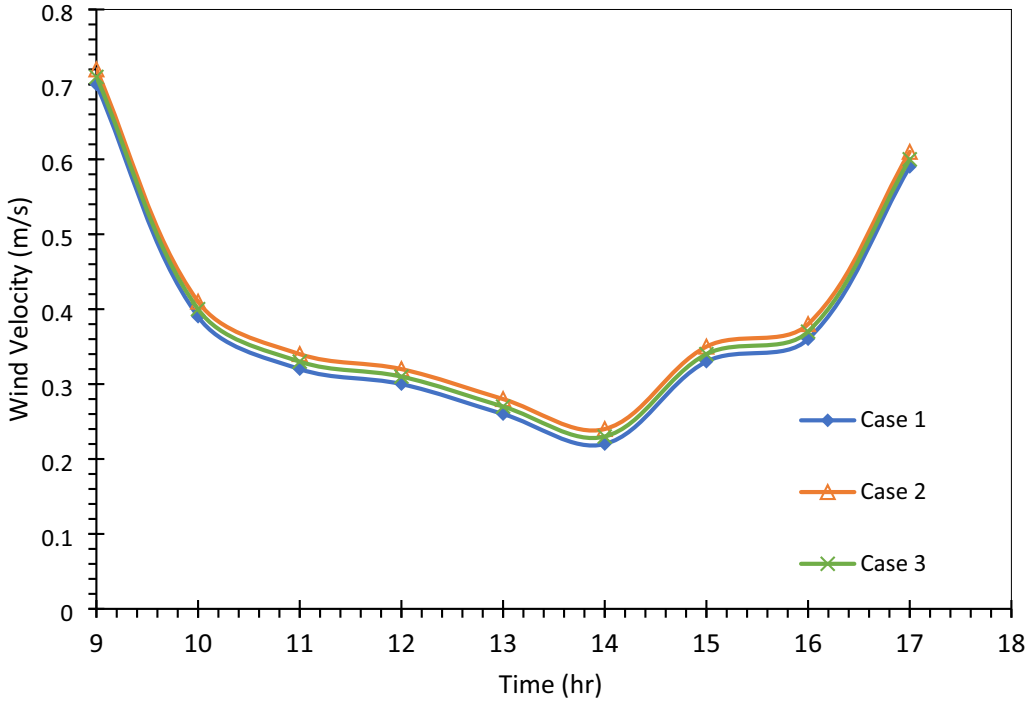

Figure 7. Wind velocity during experimentation.

was found to be lowest in case 2 i.e., 59.28°C; however, in Case 3, it was found 70.11°C.

The variation of outlet temperature on case 1 is 36°–60°C; 35°–58.20°C on case 2 and 38.5°–73.2°C on case 3 as presented in figure 8. The average outlet temperature was found to be lowest in case 2 i.e., 48.23°C; however, in case 3. It was found that 55.36°C. Case 3 shows superior performance due to the application of the reflector because it provides additional input energy to the solar air heater.

Thermal efficiency and exergy efficiency depend on global solar radiation. The variation of global solar radiation, thermal efficiency and exergy efficiency during experimentation in all three cases is shown in figure 9. Experiment was conducted from 9.00 AM to 5.00 PM in all three cases on 10–12 April 2020. The variation of solar radiation on case 1 is 360–950 W/m^2; 355–945 W/m^2 on case 2 and 350–940 W/m^2 on case 3 as presented. In all three cases, the maximum solar radiation comes out at 1.00 PM and minimum at 5.00 PM. Hence average variation in global radiation is less than 1% among all three cases of experimentation.

Based on experimental results, thermal energy and exergy efficiencies are evaluated.

The variation of thermal efficiency on case 1 is 7.16–19.67 %; 43.2–66.13 % on case 2 and 54.08–75.92 % on case 3 as presented in figure 9. Average thermal efficiency was found to be lowest in case 1 i.e., 14.21 %; however,in case 3, it was found that 65.05%.

The variation of exergy efficiency on case 1 is 1.15–3.57%; 6.97–12.48% on case 2 and 10.28–21.83 % on case 3, as presented in figure 9. The average exergy efficiency was found to be lowest in the case 1 i.e., 2.2 %; however, in case 3, it was found to be 17.61 %. Case 3 shows superior performance due to the application of the reflector because it provides additional input energy to the solar air heater.

3.2 *Validation*

Esen *et al* [16] studied the double pass solar heater. The absorber plate of the system was made of aluminium cane. The maximum solar radiation was found to be 1003 W/m^2. Proposed system with reflector, the maximum solar radiation was found to be 940 W/m^2. All other parameters are dependent on solar radiation. Both ambient conditions were almost similar, with less than 10% increase or decrease. The peak outlet temperature of the referred system is 68°C; however, for the proposed system, the peak temperature is 73.5°C under same mass flow rate (0.025 kg/s). The peak temperature of the referred system was found to be 37.1°C and 37.18°C for the proposed system. Both systems had same dimension and absorber plate area. The peak thermal efficiency of the referred system was found to be 59.65% at 1.00 PM. However, 65.05 % was found for the proposed system. Hence the proposed system shows higher thermal performance than the other types of double pass solar air

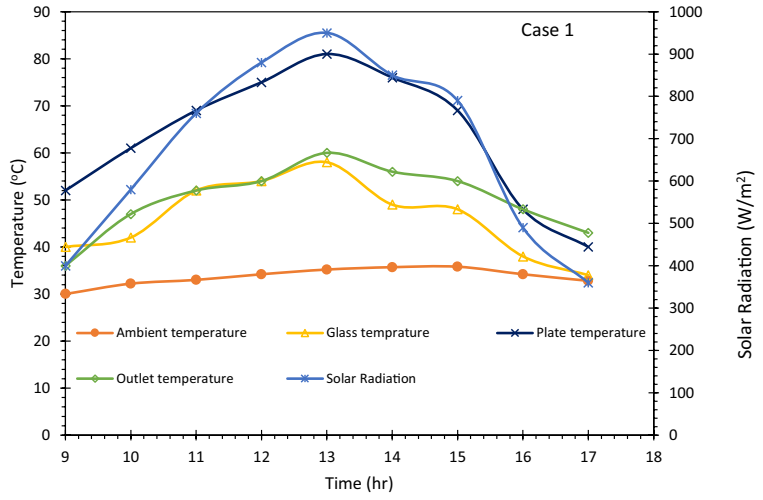

(**a**) Case 1

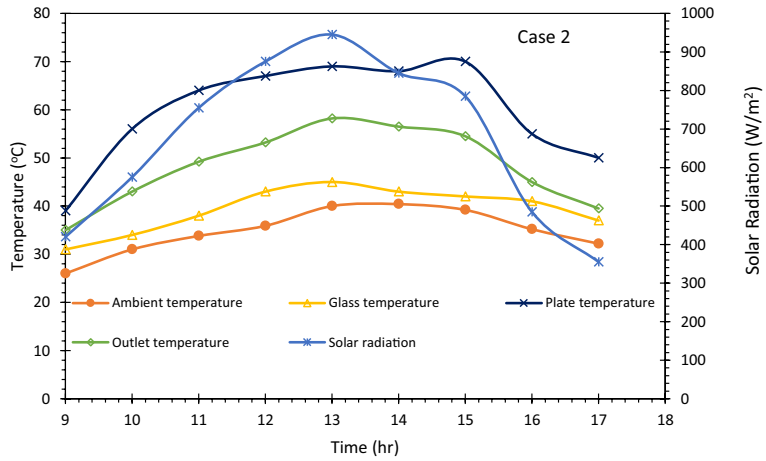

(**b**) Case 2

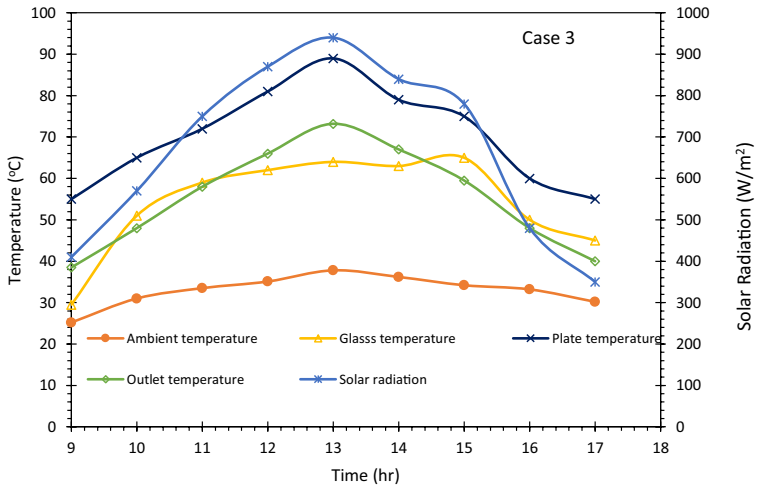

(**c**) Case 3

Figure 8. Temperature and Solar radiation during experimentation in all cases.

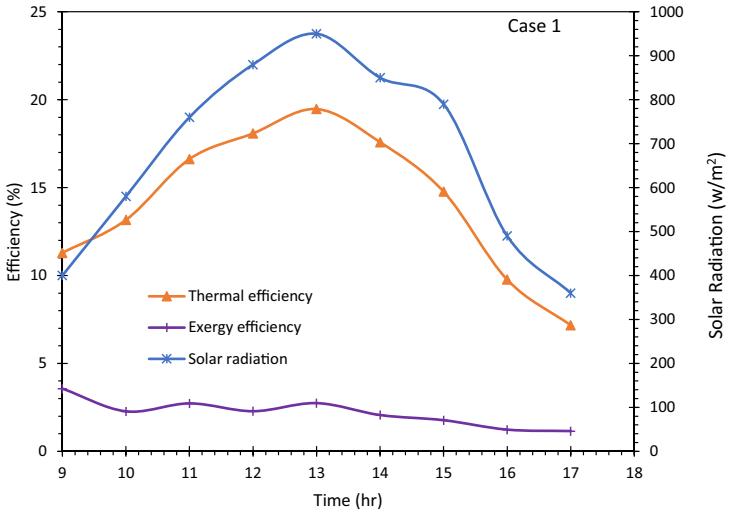

(a) Case 1

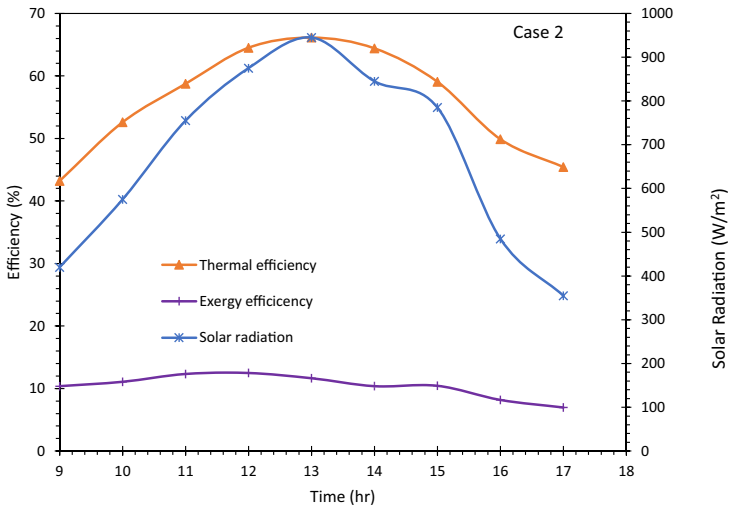

(b) Case 2

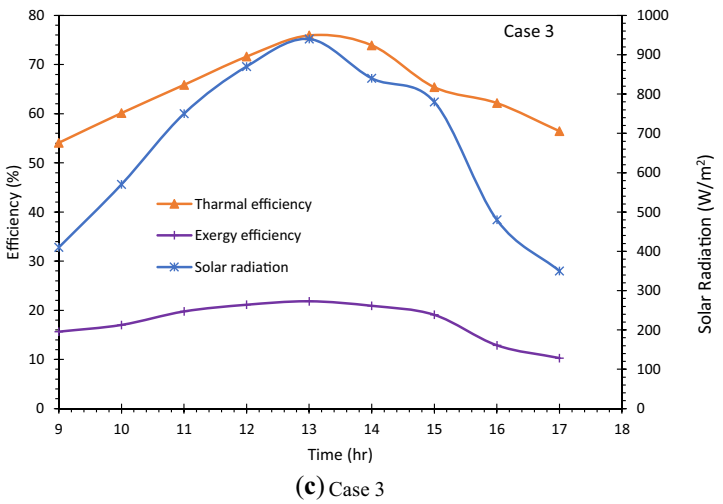

(c) Case 3

Figure 9. Efficiency and Solar radiation during experimentation in all cases.

heater. This is mainly due to reflector and thermal storage material.

4. Conclusion

A sensible heat storage based double pass hybrid solar air heater with and without reflector was experimentally investigated. Following conclusions could be drawn from this study.

1. The system is designed to have double pass type. Here black coated aluminum sheet is used as absorber sheet and Metco material and aluminum scrap mixture is used as sensible heat storage material which is applied under the bottom layer. Steel reflector is applied in the solar air heater to provide additional input energy.
2. Global solar radiation is the most important ambient parameters. In all three cases have almost similar variation. The variation of solar radiation on case 1 is 360–950 W/m^2; 355–945 W/m^{2}on case 2 and 350–940 W/m^{2}on case 3.
3. The outlet temperature of the system in case 1 shown highest temperature as compared to case 1 and 2. All three cases were experimented under almost similar atmospheric conditions. Air mass flow rate for case 2 and 3 was 0.025 kg/s. The outlet temperature varies from in case 3 was 38.5°–73.2°C and average temperature was 55.36°C.
4. The variation of thermal efficiency on case 1 is 7.16–19.67 %; 43.2–66.13 % on case 2 and 54.08–75.92 % on case 3. The average thermal efficiency was found to be lowest in case 1 i.e., 14.21 %; however, in case 3, it was found that 65.05 % on case 3. This was mainly due to application of the reflector. It provided additional input energy to the solar air heater.
5. The variation of exergy efficiency on case 1 is 1.15–3.57 %; 6.97–12.48 % on case 2 and 10.28–21.83 % on case 3. Average exergy efficiency was found to be lowest in case 1 i.e., 2.2%; however, in case 3, it was found that 17.61 % on case 3.
6. This was mainly due to application of the reflector. It provided additional input energy to the solar air heater.

The proposed solar air heater can be effectively used for industrial and domestic applications such as drying, space heating, desalination, etc.

List of symbols

Q_A	Total heat (W)
Q_u	Heat utilized (W)
Q_{loss}	Heat loss (W)
Q_{st}	Incident heat energy stored in the heater area (W)
$\dot{m}$	Mass flow rate (MFR), kg/s
C_p	Specific Heat in constant pressure (J/kg.K)
T_{out}	Outlet Temperature (^{o}C)
T_{inlet}	Inlet Temperature (^{o}C)
V_{air}	Velocity of air (m/s)
S	Area of the duct (m^2)
A_{plate}	Area of Absorber Plate (m^2)
I_i	Solar radiation (W/m^2)
U_{loss}	Overall heat loss coefficient [W/(m^{2}K)]
T_{plate}	Absorber plate temperature (^{o}C)
$T_{ambient}$	Ambient Temperature (^{o}C)
U_{side}	Side heat loss coefficient [W/(m^{2}K)]
U_{bot}	Bottom heat loss coefficient [W/(m^{2}K)]
U_{top}	Top heat loss coefficient [W/(m^{2}K)]
$h_{r,Pg}$	Radiative heat transfer coefficient (Wm^{-2}K^{-1})
$h_{c,Pg}$	Convective heat transfer coefficient (Wm^{-2}K^{-1})
$h_{r,ga}$	Radiative heat transfer coefficient due to wind velocity (Wm^{-2}K^{-1})
h_w	External radiative and convective heat transfer coefficient due to velocity of wind (Wm^{-2}K^{-1})
Nu	Nusselt Number
Ra	Reynolds number
Pr	Prandtl number
t	Temperature (^{o}C)
T_{ground}	Temperature of glass plate (^{o}C)
$T_{ambient}$	Ambient Temperature (^{o}C)
ε_{plate}	Emissivity of the plate
T_{sky}	Temperature of the external air at the surrounding (^{o}C)
L_1	Length of Solar air heater(m)
L_2	Width of solar air heater (m)
L_3	Height of the solar air heater(m)
g	Gravitation constant (m^3 kg^{-1} s^{-2})
ΔT	Temperature difference of air, (^{o}C)
L	Length of the solar air heater (m)
v	Kinematic viscosity of air (J)
D_h	Characteristic distance (m)
Ex_{inlet}	Exergy at entrance (J)
Ex_{dest}	Exergy destroyed (J)
Ex_{outlet}	Exergy at outlet(J)
Ex_{stored}	Exergy stored (J)
Ex_{lost}	Exergy lost(J)
P_{inlet}	Air Pressure inside solar air heater[kg/(mS^2)]
P_{amb}	Atmospheric Pressure [kg/(mS^2)])
T_s	Mean temperature of the absorber plate (^{o}C)
r	Distribution of solar radiation
A_{col}	Area of the collector (m^2)
$Ex_{dest(p-s)}$	Exergy destroyed due to pressure drop (J)
$\eta_{thermal}$	Thermal Efficiency
η_{exergy}	Exergy Efficiency
$Ex_{dest(\Delta P)}$	Exergy destroyed from absorber plate to surrounding (J)

ΔP	Pressure drop [kg/(mS^2)]
$Ex_{dest(p-f)}$	Exergy destroyed from absorber plate surface to flowing air (J)
W_Y	Uncertainty analysis due to anomalous system
$W_{Temperature}$	Uncertainty analysis due to temperature measuring instrument
$W_{thermometer}$	Error due to thermometer
$W_{reading}$	Reading error
W_{Wind}	Temperature error due to wind speed
$W_{anemometer}$	Error due to wind speed and pressure
W_{SR}	System deformities error
$W_{Pyranometer}$	Error in solar irradiance on a planar surface
$W_{Experimental}$	Experimental error

Greek symbols

α	Absorptivity
ρ	Density of air (kg/m^3)
ε_g	Emissivity of glass surface
λ	Insulation thermal conductivity (W/mK)
λ_e	Insulation thermal conductivity at the side (W/mK)
δ_{bot}	Insulation thickness at the bottom(mm)
δ_e	Insulation thickness at the side (mm)
σ	Stefan–Boltzmann Constant (W/m^2 K^4)
τ	Transmissivity
μ	Air viscosity (Ns/m^2)
β	Thermal expansion coefficient

References

[1] Ahmad A, Prakash O, Kumar A and Pandey A 2020 A Review of Solar Air Heater. *Low Carbon Energy Supply Technologies and Systems*. 1:1-10

[2] Benli H 2013 Experimentally derived efficiency and exergy analysis of a new solar air heater having different surface shapes. *Renew. Energy* 50: 58–67

[3] Abo-Elfadl S, Hassan H and El-Dosoky M F 2020 Study of the performance of double pass solar air heater of a new designed absorber: an experimental work. *Sol. Energy* 198: 479–489

[4] Abo-Elfadl Saleh, Yousef Mohamed S and Hassan Hamdy 2021 Energy, exergy, and enviroeconomic assessment of double and single pass solar air heaters having a new design absorber. *Process Saf. Environ. Protect.* 149: 451–464

[5] Bensaci C E, Moummi A, Sanchez de la Flor F J, Rodriguez Jara E A, RinconCasado A and Ruiz-Pardo A 2020 Numerical and experimental study of the heat transfer and hydraulic performance of solar air heaters with different baffle positions. *Renew. Energy* 155: 1231–1244

[6] Satcunanathan S and Deonarine S 1973 A two-pass solar air heater. *Sol. Energy* 15(1): 41–49

[7] Kumar A, Singh A P and Singh O P 2020 Efficient designs of double-pass curved solar air heaters. *Renew. Energy* 160: 1105–1118

[8] Yeh H M, Ho C D and Hou J Z 2002 Collector efficiency of double-flow solar air heaters with fins attached. *Energy* 27(8): 715–727

[9] Ho C, Chang H, Wang R and Lin C 2012 Performance improvement of a double-pass solar air heater with fins and baffles under recycling operation. *Appl. Energy* 100: 155–163

[10] Baig W and Ali H M 2019 An experimental investigation of performance of a double pass solar air heater with foam aluminum thermal storage medium. *Case Stud. Thermal Eng.* 14: 100440

[11] Vijayan S, Arjunan T V, Kumar A and Matheswaran M M 2020 Experimental and thermal performance investigations on sensible storage based solar air heater. *J. Energy Storage* 31: 101620

[12] Kalaiarasi G, Velraj R, Vanjeswaran M N and Pandian N G 2020 Experimental analysis and comparison of flat plate solar air heater with and without integrated sensible heat storage. *Renew. Energy* 150: 255–265

[13] Aboul-Enein S, El-Sebaii A A, Ramadan M R I and El-Gohary H G 2000 Parametric study of a solar air heater with and without thermal storage for solar drying applications. *Renew. Energy* 21(3–4): 505–522

[14] Duffie J A, Beckman W A and Blair N 2020 Solar engineering of thermal processes, photovoltaics and wind. John Wiley & Sons

[15] Nidhul K, Yadav A K, Anish S and Arunachala U C 2020 Efficient design of an artificially roughened solar air heater with semi-cylindrical side walls: CFD and exergy analysis. *Sol. Energy* 207: 289–304

[16] Esen H 2008 Experimental energy and exergy analysis of a double-flow solar air heater having different obstacles on absorber plates. *Build. Environ.* 43(6): 1046–1054

[17] Rhee S J and Edwards D K 1981 Laminar entrance flow in a flat plate duct with asymmetric suction and heating. *Numer. Heat Transfer* 4(1): 85–100

[18] Bouadila S, Lazaar M, Skouri S, Kooli S and Farhat A 2014 Energy and exergy analysis of a new solar air heater with latent storage energy. *Int. J. Hydrog. Energy* 39(27): 15266–15274

[19] Kurtbas I and Durmuş A 2004 Efficiency and exergy analysis of a new solar air heater. *Renew. Energy* 29(9): 1489–1501

[20] Abuşka M 2018 Energy and exergy analysis of solar air heater having new design absorber plate with conical surface. *Appl. Thermal Eng.* 131: 115–124

[21] Acır A, Canlı M E, Ata İ and Sakıroğlu R 2017 Parametric optimization of energy and exergy analyses of a novel solar air heater with grey relational analysis. *App. Thermal Eng.* 122: 330–338

[22] Matheswaran M M, Arjunan T V and Somasundaram D 2018 Analytical investigation of solar air heater with jet impingement using energy and exergy analysis. *Sol. Energy* 161: 25–37

[23] Alta D, Bilgili E, Ertekin C and Yaldiz O 2010 Experimental investigation of three different solar air heaters: energy and exergy analysis. *Appl. Energy* 87(10): 2953–2973

[24] Ghaderian J, Azwadi C N and Mohammed H 2015 Modelling of energy and exergy analysis for a double-pass solar air heater system. *J. Adv. Res. Fluid Mech. Thermal Sci.* 16: 15–32

[25] Koroneos C, Nanaki E and Xydis G 2010 Solar air conditioning systems and their applicability—an exergy approach. *Resour. Conserv. Recycl.* 55(1): 74–82

[26] Kumar A, Saini R P and Saini J S 2014 A review of thermohydraulic performance of artificially roughened solar air heaters. *Renew. Sustain. Energy Rev.* 37: 100–122

[27] Prakash O and Kumar A 2017 Solar drying technology: concept, design, testing, modeling, economics, and environment. Springer

[28] Menni Y, Azzi A and Chamkha A 2019 The solar air channels: comparative analysis, introduction of arc-shaped fins to improve the thermal transfer. *J. Appl. Comput. Mech.* 5(4): 616–626

[29] Öztürk H H 2005 Experimental evaluation of energy and exergy efficiency of a seasonal latent heat storage system for greenhouse heating. *Energy Convers. Manag.* 46(9–10): 1523–1542

[30] Phu N M and Luan N T 2020 A review of energy and exergy analyses of a roughened solar air heater. *J. Adv. Res. Fluid Mech. Thermal Sci.* 77(2): 160–175